Ceramide regulation of nuclear protein import[S]

Randolph S. Faustino, Paul Cheung, Melanie N. Richard, Elena Dibrov, Annette L. Kneesch, Justin F. Deniset, Mirna N. Chahine, Kaitlin Lee, David Blackwood, and Grant N. Pierce[1]

Institute of Cardiovascular Sciences, St. Boniface Hospital Research Centre, Department of Physiology, Faculties of Medicine and Pharmacy, University of Manitoba, Winnipeg, Manitoba, Canada

Abstract **Nucleocytoplasmic trafficking is an essential and responsive cellular mechanism that directly affects cell growth and proliferation, and its potential to address metabolic challenge is incompletely defined. Ceramide is an antiproliferative sphingolipid found within vascular smooth muscle cells in atherosclerotic plaques, but its mechanism of action remains unclear. The hypothesis that ceramide inhibits cell growth through nuclear transport regulation was tested. In smooth muscle cells, exogenously supplemented ceramide inhibited classical nuclear protein import that involved the activation of cytosolic p38 mitogen-activated protein kinase (MAPK). After application of SB 202190, a specific and potent pharmacological antagonist of p38 MAPK, sphingolipid impingement on nuclear transport was corrected. Distribution pattern assessments of two essential nuclear transport proteins, importin-α and Cellular Apoptosis Susceptibility, revealed ceramide-mediated relocalization that was reversed upon the addition of SB 202190. Furthermore, cell counts, nuclear cyclin A, and proliferating cell nuclear antigen expression, markers of cellular proliferation, were diminished after ceramide treatment and effectively rescued by the addition of inhibitor. Together, these data demonstrate, for the first time, the sphingolipid regulation of nuclear import that defines and expands the adaptive capacity of the nucleocytoplasmic transport machinery.**—Faustino, R. S., P. Cheung, M. N. Richard, E. Dibrov, A. L. Kneesch, J. F. Deniset, M. N. Chahine, K. Lee, D. Blackwood, and G. N. Pierce. **Ceramide regulation of nuclear protein import.** ***J. Lipid Res.*** **2008.** 49: **654–662.**

Supplementary key words nuclear transport • lipid • mitogen-activated protein kinase

Synthesized in the sphingolipid pathway from serine and palmitoyl-CoA (1) or generated by sphingomyelinase activity (2), ceramide is an important second messenger that primarily stimulates apoptosis and growth arrest (3, 4). Reported to induce a significant antiproliferative effect in vascular smooth muscle cells (VSMCs) (5, 6), the mechanism whereby ceramide affects cellular proliferation has not been fully elucidated.

Proliferation and growth are regulated by nuclear transport (7, 8). An essential eukaryotic process, nucleocytoplasmic transport, describes the regulated movement of molecules between nuclear and cytoplasmic compartments (9, 10), defined by cytosolic (11, 12) and membrane-bound (13–15) phases, that characterize the distribution of the nuclear transport machinery. Classical nuclear import involves proteins that bear a monopartite or bipartite polybasic amino acid sequence [nuclear localization signal (NLS)] (16). Transport is initiated upon energy-independent NLS recognition by a heterodimeric NLS receptor (17, 18) composed of an α subunit (importin-α), which recognizes the NLS (19), and a β subunit (20) (importin-β), which mediates nuclear pore complex docking at the nuclear envelope (21–23). Translocation of the NLS-receptor assembly through the nuclear pore complex is an energy-dependent process (24–26) controlled by a RanGTP/GDP cycle (27–29). Importin-α is returned to the cytosol by CAS (for Cellular Apoptosis Susceptibility), a nuclear export protein specific for the α subunit (30). Importin-β is recycled independently of the α subunit, and the NLS bearing protein cargo is released into the nuclear interior to modulate gene expression and growth (28).

Nuclear protein import is one step in a complex series of events that ultimately leads to cell growth. In this study, we investigated the potential for antiproliferative effects of ceramide in VSMCs to be mediated through an action on nuclear protein import. Although overt changes in nucleocytoplasmic trafficking will dramatically affect cellular homeostasis, it is unclear whether subtle stimuli can sufficiently alter transport to effect physiological and pathological changes in cell growth. Although metabolism plays an important role in modifying nuclear protein import (31), it currently remains unknown whether a lipid metabolite can inhibit nuclear transport. This suggestion was based upon an association of nuclear pore density with cellular transcriptional capacity and "release of products to the cytoplasm" (31). More recently, it was shown that phosphorylation plays an important regulatory role in nuclear protein import (32, 33). However, little is known concerning the direct modulatory effects of specific lipid metabolism

Manuscript received 12 October 2007 and in revised form 11 December 2007.

Published, JLR Papers in Press, December 14, 2007.
DOI 10.1194/jlr.M700464-JLR200

[1] To whom correspondence should be addressed.
e-mail: gpierce@sbrc.ca

[S] The online version of this article (available at http://www.jlr.org) contains supplementary data in the form of two figures.

molecules on nuclear protein import within a cell. This is particularly important in vascular diseases like atherosclerosis and hypertension, in which lipids, cell growth, and cell proliferation play important pathogenic roles. Here, ceramide demonstrates a capacity to induce strong inhibitory effects on nuclear protein import, ultimately reflecting changes in cellular growth and proliferative capacity.

MATERIALS AND METHODS

Materials

DMEM, FBS, and Fungizone were purchased from Gibco BRL. Ceramide was purchased from Biomol. Recombinant p38 mitogen-activated protein kinase (MAPK), SB 202190, SB 203580, and Fluorsave were from Calbiochem. Alexa-BSA as well as the Alexa-conjugated goat anti-mouse secondary antibody were purchased from Molecular Probes. Primary antibodies for CAS and importin-α were purchased from BD Transduction Laboratories, phospho-p38 and p38 MAPK were purchased from Cell Signaling, proliferating cell nuclear antigen (PCNA) antibody was purchased from Sigma-Aldrich, and GAPDH and cyclin A antibodies were purchased from Abcam. All other chemicals were purchased from Sigma-Aldrich Canada.

Cell culture

VSMCs were cultured from thoracic aorta explants isolated from New Zealand White rabbits as described previously (29, 32, 33). Cells were seeded on acid-rinsed coverslips at initial seeding densities of 2.0×10^5 or 1.9×10^5 cells/coverslip and starved for 3 days, then fed with DMEM containing 5% FBS +

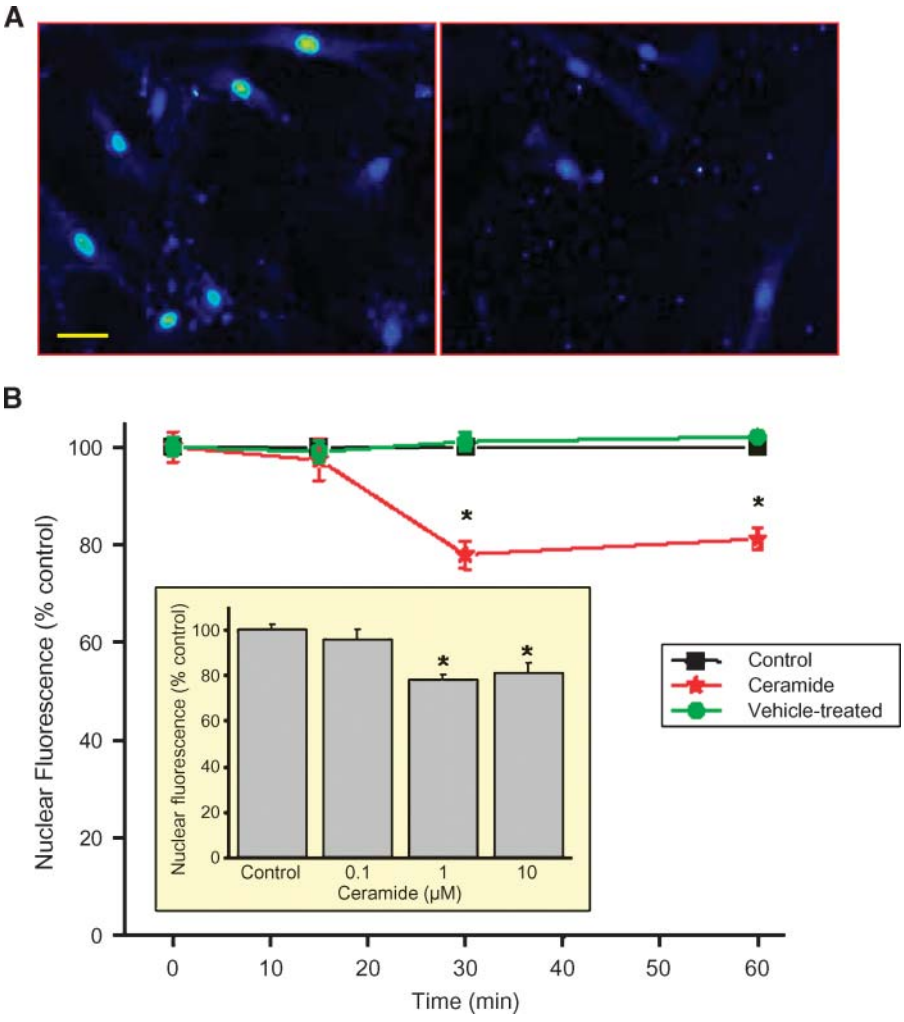

Fig. 1. Treatment of vascular smooth muscle cells (VSMCs) with ceramide causes a time-dependent decrease in nuclear import. Nuclear import mix with or without 1 μM ceramide was used in import studies on VSMCs. A: Nuclear fluorescence was quantitated in control (left) and ceramide-treated (right) cells. Bar length = 40 μM. B: Pretreatment of cytosol with 1 μM ceramide significantly decreased nuclear protein import after 30 min when normalized to controls and was sustained over the course of 1 h. Pretreatment of cytosol with vehicle (DMSO) had no effect. Values shown are means ± SEM. * $P < 0.05$, n = 3 (sample ~ 100 cells). Inset: Ceramide pretreatment for 30 min caused a dose-dependent inhibition of nuclear protein import. VSMCs supplemented with 0.1 μM ceramide had no significant effect. Treatment with 1 and 10 μM ceramide significantly inhibited nuclear protein import. Values shown are means ± SEM. * $P < 0.05$ versus control, n = 3 (sample composed of ~60–120 cells).

2% Fungizone at 24 h before use in the nuclear import assay. Cells for use in microinjection were initially seeded at a density of 1.5×10^5 cells/coverslip. Cell count experiments were done by trypsinization and then counted using a hemocytometer.

Nuclear import assays

Nuclear protein import assays were performed as described previously (32, 34). Briefly, nuclear import mix containing nuclear import buffer (20 mM HEPES, 110 mM K^+ acetate, 5 mM Na^+ acetate, 2 mM Mg^{2+} acetate, and 0.5 mM EGTA, pH 7.5) and 50% rat liver cytosol was treated with 0.1, 1, and 10 μM ethanol-solubilized ceramide to examine dose-dependence. Nuclear import mix was treated with 1 μM ceramide for 15, 30, and 60 min to examine time-dependent effects of ceramide treatment. If present, 1 μM SB 202190 was added to the nuclear import mix before use in the nuclear import assay. Exogenous recombinant p38 MAPK was added at a final concentration of 4 μg/ml with or without 1 μM SB 202190 and preincubated with nuclear import mix for 30 min at 37°C before use in the nuclear import assay. To prepare VSMCs for the transport assay, cells were permeabilized with 40 μg/ml digitonin and rinsed three times with 1× PBS after 5 min. Nuclear import was initiated by inverting coverslips with permeabilized VSMCs onto 50 μl drops of treated import mix plus 5 μl of fluorescent substrate in a humidified Parafilm-lined box and incubated at 37°C. The fluorophore used in this study was BSA conjugated to Alexa 488, which was subsequently cross-linked to a synthesized NLS (CGGGPKKKRKVED), resulting in the Alexa-BSA-NLS substrates used in our experiments. After import, cells were fixed with 3.7% paraformaldehyde for 15 min and subsequently visualized on a Bio-Rad MRC600 confocal laser scanning microscope using the 488 nm laser line and the VHS filter block. Nuclear fluorescence was assessed using Molecular Dynamics Imagespace 3.2.1 software on a Silicon Graphics O_2 Workstation, and images were processed using Confocal Assistant version 3.0.

Microinjection

Coverslips containing VSMCs were placed in a Leyden dish, and 1 ml of prewarmed perfusate buffer (6 mM KCl, 1 mM $MgCl_2$, 1 mM $CaCl_2$, 10 mM dextrose, and 6 mM HEPES, pH 7.4) was added (35). Temperature was maintained at 37°C in a microperfusion chamber. Approximately 10 μl of fluorescent substrate (Alexa-BSA-NLS) in nuclear import buffer + ceramide (for a final concentration of 1 μM ceramide) was added to a micropipette using a 1 ml syringe, ensuring that no bubbles were present in the tip. Cells exhibit a small degree of autofluorescence that allow the visualization of the cell before injection. Using an MS314 micromanipulator (Fine Science Tools), the pipette was inserted

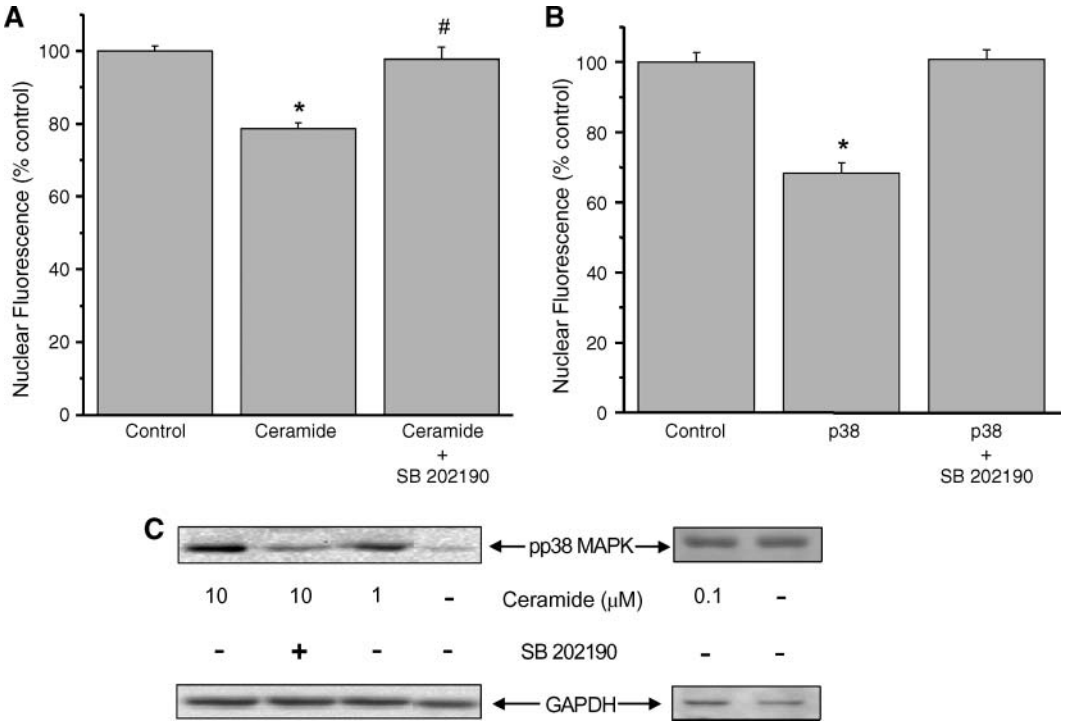

Fig. 2. Involvement of mitogen-activated protein kinase (MAPK) in ceramide-mediated inhibition of nuclear protein import. A: Inhibition of nuclear protein import by a specific inhibitor of the p38 MAPK pathway. Nuclear import mix was treated with 1 μM ceramide with or without 1 μM SB 202190 for 30 min. Treatment with SB 202190 significantly reversed the ceramide-dependent inhibition of nuclear protein import. Values shown are means ± SEM. * $P < 0.05$ versus control, n = 3; # $P < 0.05$ versus ceramide, n = 3 (~100 cells were examined in each separate experiment). B: Treatment of nuclear protein import mix with exogenous p38 MAPK inhibits nuclear protein import in a reversible manner. VSMCs were incubated with nuclear import mix pretreated with exogenous p38 MAPK with or without 1 μM SB 202190. Treatment with p38 MAPK alone significantly inhibited nuclear protein import and was reversed upon addition of 1 μM SB 202190. Values shown are means ± SEM. * $P < 0.05$, n = 3 (sample composed of ~90 cells studied). C: Dose-dependent effect of ceramide on the phosphorylation of p38 MAPK. Rat hepatocyte lysate was treated with phosphorylation mix, and ceramide was added at 0.1, 1, and 10 μM. Immunoblot analysis was performed with anti-phospho-p38 MAPK antibody. Control samples were prepared using phosphorylation mix without ceramide. Minimal phosphorylated p38 MAPK was observed in control samples, whereas phosphorylation of p38 MAPK was increased significantly with 1 and 10 μM ceramide treatment. No activation was observed with 0.1 μM. Dose-dependent phosphorylation was inhibited by the p38 MAPK-specific inhibitor SB 202190. Equal sample loading was confirmed by GAPDH detection (lower panel).

into the cell cytoplasm in close proximity to the nucleus. The PV830 Pneumatic PicoPump microinjector (World Precision Instruments) was used with the following settings: injection hold pressure, 40 p.s.i.; eject pressure, 60 p.s.i.; range, 100 ms; period, 80. Cells were injected four times, and the pipette was slowly removed from the cell. Images of the microinjected cell were acquired on a Bio-Rad MRC600 confocal laser scanning microscope as described for the nuclear import assays. Images were taken of preinjection and postinjection cells followed by set time points to observe the rate of nuclear import for each cell over time.

Immunofluorescent staining

Cells and nuclear import mix were prepared as described for the nuclear import assay, with minor modifications. For these experiments, the Alexa-BSA-NLS substrate was not included, and after cells were fixed with 3.7% paraformaldehyde, they were permeabilized with 0.1% Triton X-100 and then incubated in blocking buffer (1× PBS, 2% skim milk, and 0.1% Tween-20) for 30 min at room temperature. Coverslips were washed three times with wash buffer (1× PBS and 1% skim milk) and inverted on 50 μl of wash buffer containing a 1:10 dilution of anti-CAS or anti-importin-α in a Parafilm-lined box. For the determination of cyclin A distribution, coverslips were incubated with a 1:50 dilution of cyclin A primary antibody. Coverslips were incubated for 1 h at room temperature, washed three times, and then incubated with a 1:1,000 dilution of Alexa-conjugated goat anti-mouse secondary antibody for 1 h. Coverslips were rinsed with 1× PBS and mounted on glass slides using Fluorsave. After drying, cells were visualized using a 40× objective lens and a 488 nm filter block on a Zeiss Axioskop 2 MOT microscope. Images were captured using a Zeiss Axiocam and pseudocolored using Axiovision Viewer version 3.0. Mean pixel values represent fluorescent intensity and were assessed using Molecular Dynamics Imagespace software; they range on a scale from 0 to 255, with 0 for no fluorescence and 255 indicating complete saturation. Nuclear rim accumulation was determined by restricting area measurements to spaces immediately adjacent to the nuclear envelope.

Western blot analysis

Rat liver extract was examined for MAPK activation as a function of exposure to ceramide. Briefly, a phosphorylation mix (including ATP, creatine phosphate, and creatine phosphokinase) was added to the rat liver cytosolic extract at 25°C and incubated for 2 min before the addition of ceramide at the indicated dosage. A further 11 min of incubation at 37°C was performed before the addition of sample loading buffer. The final reaction mix was separated by electrophoresis, and the proteins were semi-dry-transferred onto nitrocellulose membranes. Primary antibody for phosphorylated p38 MAPK (pp38 MAPK) was added at 1:1,500 in 1% milk. Cell lysates were also examined for PCNA protein expression with a 1:3,000 dilution of anti-PCNA primary antibody. Standard secondary goat anti-mouse incubation and ECL fluorescence imaging were also performed.

Statistics

Results are reported as means ± SEM, analyzed by one-way ANOVA followed by Duncan's post hoc test, and significance was set at $P < 0.05$. For permeabilized cell nuclear import assays, n was taken to be one trial, where each trial consisted of 60–120 cells.

RESULTS

Ceramide inhibits nuclear import through the p38 signaling axis

The nuclear accumulation of fluorescent reporter substrate in VSMCs was attenuated compared with that in untreated controls after ceramide treatment (**Fig. 1A**). In-

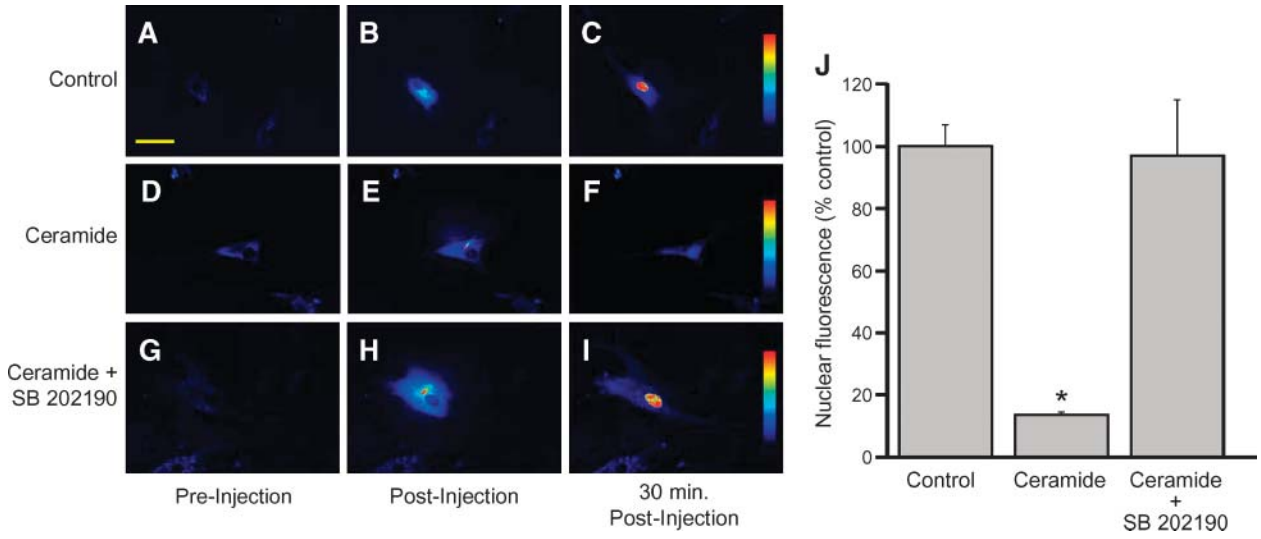

Fig. 3. Microinjection of smooth muscle cells with ceramide inhibits nuclear localization of import substrate. VSMCs were microinjected with injection buffer containing Alexa-BSA-nuclear localization signal (NLS), and images were taken before injection, immediately after injection, and 30 min after injection. Note the low autofluorescence in preinjection cells (A, D, G). Images of cells immediately after injection in some cases show the micropipette tip containing fluorescent import substrate (E, H). Control cells are shown after injection after removal of the micropipette (B) and microinjected with import substrate, which sustained a peak nuclear fluorescence after 30 min (C). Addition of ceramide to injection buffer significantly inhibited the nuclear localization of the Alexa-BSA-NLS substrate (F). Nuclear import of fluorophore was restored in cells injected with ceramide + 1 μM SB 202190 (I). The color scale indicates the measure of fluorescence, where blue and red represent low and high intensities, respectively. Bar length for Panel A = 40 μM. Results from several experiments are depicted in bar graph format in J. Values shown are means ± SEM. * $P < 0.05$ versus control, n = 3.

hibition of import was first observed after 30 min of pretreatment with 1 μM ceramide, whereas untreated control and vehicle-treated cells showed no significant changes in maximal nuclear fluorescence over 60 min (Fig. 1B). Although 1 μM ceramide was sufficient for inhibition, other concentrations were investigated for possible effects on nuclear transport. Addition of 0.1 μM showed no statistically significant differences compared with untreated control cells, whereas 1 and 10 μM demonstrated similar effects on nucleocytoplasmic transport (Fig. 1B, inset).

MAPK-mediated decreases in nuclear import have been reported previously (32, 35, 36). The p38 MAPK inhibitor, SB 202190, was included with ceramide when pretreating cytosol to investigate the participation of p38 signaling. Although treatment with SB 202190 alone or DMSO vehicle had no effects on nuclear import (data not shown), nuclear fluorescence of ceramide-treated cells was restored to baseline levels when supplemented with pharmacological antagonist (**Fig. 2A**). Specific effects of p38 MAPK were assessed by incubation of permeabilized cells with active, recombinant p38 MAPK. Rates of nuclear import, decreased by 30% with enzyme alone, were restored to control levels in the presence of SB 202190 (Fig. 2B). Immunoblot analysis confirmed the presence and activation of endogenous cytosolic p38 after ceramide treatment, which was reversed after incubation with SB 202190 (Fig. 2C).

Alternatively, cells were microinjected with fluorescent substrate plus ceramide to investigate nuclear transport (**Fig. 3A–I**). Preinjection cells displayed minimal to no endogenous fluorescence (Fig. 3A, D, G), with fluorescent reporter substrate demonstrating identifiable localization in and around the microinjection site immediately after application (Fig. 3B, E, H). At 30 min after injection, nuclear fluorescence in the presence of ceramide was inhibited compared with control treatment (Fig. 3C, F), with transport levels restored to baseline upon coincubation with SB 202190 (Fig. 3I). This was consistently observed with each biological replicate, with ceramide causing a reversible 85% inhibition of transport (Fig. 3J).

Relocalization of essential transport factors follows ceramide exposure

Importin-α recognizes the classical polylysine NLS construct used in the current work and is known to constitutively shuttle between nuclear and cytosolic locales. Untreated cells stained for importin-α displayed background cytoplasmic presence with stronger nuclear localization as well as identifiable nuclear envelope staining (**Fig. 4A**, left). However, pretreatment of VSMCs with 1 μM ceramide led to nuclear exclusion of importin-α, with maintenance of strong nuclear rim and cytoplasmic staining (Fig. 4A, right). Significantly, nuclear fluorescence was decreased after ceramide treatment (Fig. 4B,

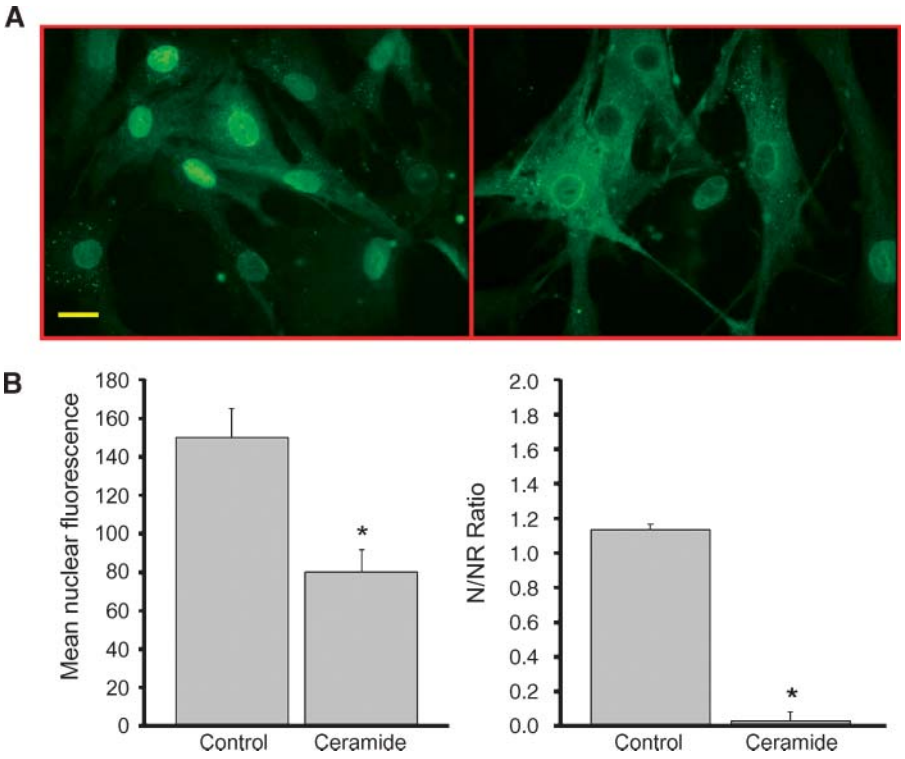

Fig. 4. Pretreatment of cells with ceramide induces the redistribution of importin-α. Cells were prepared as described for the permeabilized nuclear import assay and stained for importin-α. A: Untreated cells were used as controls and displayed constitutive nuclear localization of importin-α (left). In cells treated with 1 μM ceramide, importin-α was predominantly nonnuclear (right). Bar length = 20 μM. B: Significant decreases in mean nuclear fluorescence and nuclear/nuclear rim (N/NR) accumulation as measured in control and treated cells. Values shown are means ± SEM. * $P < 0.05$ versus control, n = 3.

left), with a concurrent shift from nuclear to nuclear rim staining (Fig. 4B, right).

CAS is an associated cofactor that exports importin-α (37). Immunocytochemistry revealed strong baseline nuclear/nuclear rim accumulation with CAS in untreated cells (**Fig. 5A**, left). Ceramide application diminished CAS staining (Fig. 5A, middle), but nuclear rim localization was restored after the addition of SB 202190 (Fig. 5A, right). Quantitative evaluation of CAS fluorescence reproducibly demonstrated the inhibition of constitutive localization after ceramide treatment, with restoration after SB 202190 supplementation (Fig. 5B, C).

Diminished proliferative capacity precipitated by ceramide

VSMC proliferation after ceramide supplementation was investigated by cell counts as well as by assessing the expression and distribution of canonical proliferative markers (see supplementary Fig. I). Treatment with 1 or 10 μM ceramide for 24 h indistinguishably and significantly diminished cell numbers. Treatment results with 10 μM ceramide are given as representative (**Fig. 6A**). This population decrease was reversed upon addition of SB 202190 or SB 203580, specific inhibitors of p38 MAPK. Cellular capacity for growth is facilitated by cyclin mobilization, and increased nuclear localization of discrete factors such as cyclin A primes the cell for a round of DNA synthesis (38). Here, untreated control nuclei clearly exhibit nuclear acquisition of cyclin A (Fig. 6B, left), whereas ceramide treatment enforces uniform cellular distribution of cyclin A without distinctive nuclear, or other, organellar compartmentalization (Fig. 6B, right).

PCNA is an alternative marker for cellular proliferation (39). Supplementing VSMC cultures with 10 μM ceramide for 24 h decreased the expression of PCNA and was effectively reversed with the addition of SB 202190 (**Fig. 7A**). Although inclusion of the pharmacological inhibitor SB 202190 together with ceramide, as well as SB 202190 alone, showed no differences compared with untreated control cells, densitometric profiling of ceramide-induced PCNA expression changes revealed a significant 25% decrease when normalized to PCNA levels in control samples (Fig. 7B).

DISCUSSION

Alterations in nuclear transport have direct consequences on cellular processes and can dictate rates of cellular growth and proliferation. Dynamic yet controlled, the nuclear transport machinery integrates various modes of regulation at multiple levels, but the participation of lipid signaling in nucleocytoplasmic traffic regulation is not fully characterized. To address this, nuclear transport was assessed in

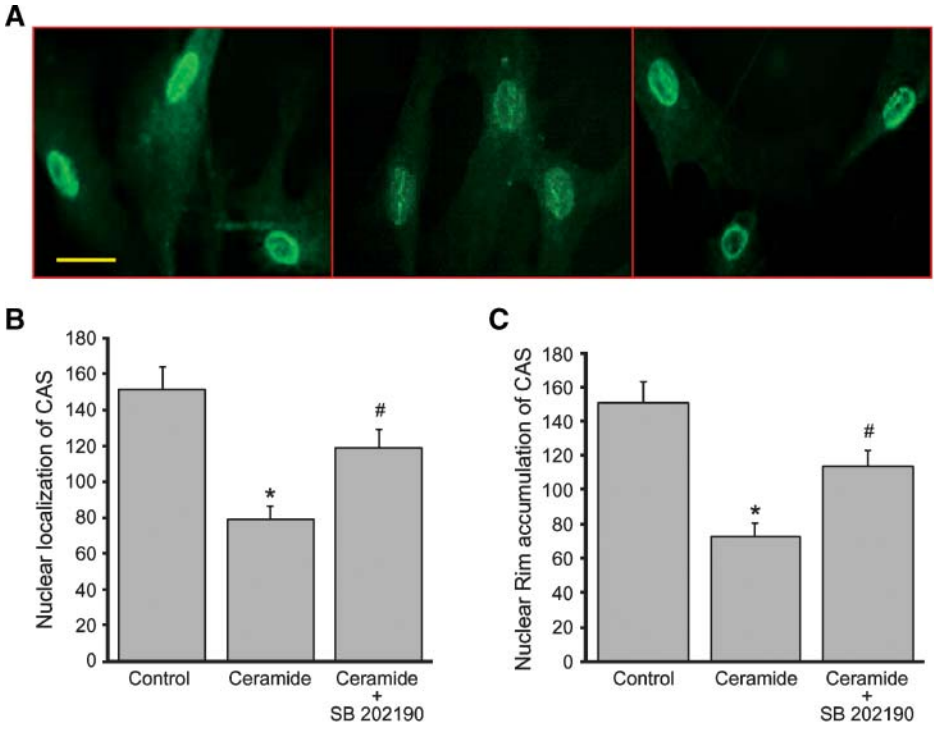

Fig. 5. Distribution of Cellular Apoptosis Susceptibility (CAS), a nuclear transport protein, is reversibly influenced by ceramide. VSMCs were prepared as described for the permeabilized nuclear import assay and subsequently fixed and stained using anti-CAS to assess the localization of CAS after ceramide treatment. A: Control cells showed a high degree of nuclear/nuclear rim staining of anti-CAS (left), which was attenuated in cells treated with 1 μM ceramide (middle). Addition of 1 μM SB 202190 in the presence of ceramide restored nuclear CAS (right). Bar length = 20 μM. B, C: Ceramide significantly inhibited nuclear, as well as nuclear rim, staining in a reversible manner. Values shown are means ± SEM. * $P < 0.05$ versus control, n = 3; # $P < 0.05$ versus ceramide, n = 3.

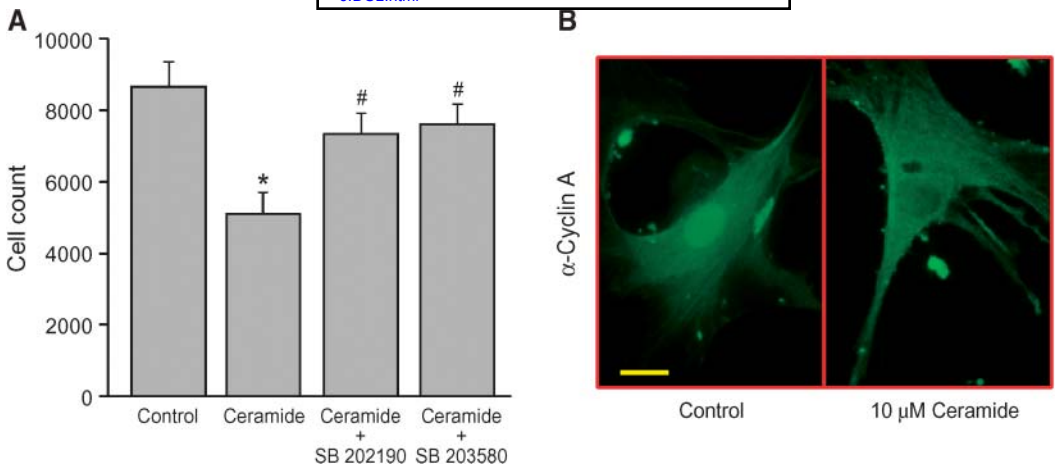

Fig. 6. Pretreatment with ceramide decreases cell proliferation and inhibits the nuclear import of cyclin A. A: Cells treated with 10 μM ceramide exhibited a significant decrease in overall cell number compared with control cells. Addition of SB 202190, as well as another highly specific p38 MAPK inhibitor, SB 203580, reversed ceramide-induced effects on cell number. Values shown are means ± SEM. * $P < 0.05$ versus control, n = 3; # $P < 0.05$ vs. ceramide, n = 3. B: Anti-cyclin A staining in VSMCs pretreated with 10 μM ceramide (left) demonstrated an overall decrease in nuclear localization compared with untreated controls (right). Bar length = 20 μM.

VSMCs in the presence or absence of sphingolipid. Here, ceramide initiated p38 signaling that attenuated classical nuclear import in VSMCs, with subsequent diminution of cellular proliferation reversed by specific pharmacological antagonism. This is the first report to link sphingolipid metabolism to nucleocytoplasmic trafficking with an ultimate impact on cellular growth.

Ceramide did not affect the import of fluorescent reporter constructs lacking the NLS (data not shown). Using cell microinjection to closely recapitulate in situ conditions, robust inhibition of nuclear protein import was observed (80%), further strengthening the relevance of this effect in VSMCs. Although these data may be interpreted as an enhancement of export, based on previous work that demonstrated ceramide augmentation of nuclear export through a Crm1/leucine-rich nuclear export signal pathway (40), the construct used in this study contains only an NLS and no export sequence. Without a nuclear export signal, ceramide could not regulate export in this study. Also, the NLS within the reporter is a "classical" sequence that does not function as an export signal. Therefore, the observed effects are attributable to changes in import rather than to export enhancement.

Nuclear import attenuation was not attributable to a nonspecific, disruptive sphingolipid-to-nuclear membrane interaction, although such an action is possible. For example, ceramide can create stable channels (41) in outer mitochondrial membranes (42), leading to increased membrane permeability. Concentrations used in the present study are below the critical threshold required to form disruptive channels, suggesting that the inhibitory capacity of ceramide was the result of specific signaling mechanisms. Furthermore, these effects were not attributable to nonspecific, general properties of all sphingolipids, as metabolites of ceramide did not possess the same potent inhibitory effects (see supplementary Fig. II). Indeed, treatment of exogenous cytosol with 10 μM sphingosine-1-phosphate in permeabilized cell assays significantly stimulated nuclear transport (see supplementary Fig. II). Sphingosine-1-phosphate and ceramide exist as oppos-

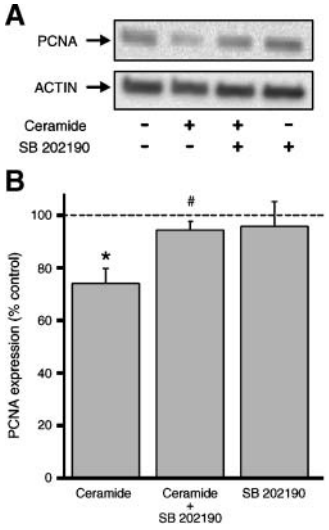

Fig. 7. Ceramide causes a reversible change in proliferating cell nuclear antigen (PCNA) expression. A: Immunoblotting with anti-PCNA revealed diminished expression of the proliferative marker in VSMCs treated with 10 μM ceramide compared with untreated conditions (first and second lanes). Treatment with ceramide + SB 202190, or with SB 202190 alone, showed no changes in PCNA expression levels, also compared with untreated cells (third and fourth lanes). Actin controls showed equal protein loading of lanes. B: Densitometric analysis identified a significant decrease in PCNA protein levels in cells treated with 10 μM ceramide when normalized to untreated cells (baseline, i.e., 100% of control, is shown as a horizontal line). Addition of SB 202190 inhibited ceramide-induced decreases in PCNA expression, and SB 202190 alone had no significant effect. Values shown are means ± SEM. * $P < 0.05$ versus control, n = 3; # $P < 0.05$ versus ceramide, n = 3.

ing sides of what is thought to be a "rheostat" mechanism, whereby sphingosine-1-phosphate stimulates cellular growth but ceramide inhibits cell growth and induces apoptosis (43–45). This augmentation of nuclear import by sphingosine-1-phosphate, therefore, is not unexpected.

Previous work has identified a MAPK-mediated inhibition of nuclear protein import by H_2O_2 (32), although a target for MAPK action remained unidentified. CAS was selected as a potential candidate for mediating the MAPK effects observed. It is a 100 kDa protein (46) intimately involved with karyopherin-dependent import (28) through its action as a nuclear exporter of importin-α (37, 47). CAS concentrations change depending on cell type as well as cellular metabolic state. For example, proliferating cells display higher levels of constitutive CAS than nonproliferating cells (48). Here, CAS was localized to the nucleus of untreated VSMCs. CAS contains a MAP kinase kinase target motif and is a physiological phosphosubstrate for MEK (49), and constitutively phosphorylated CAS is localized predominantly to the cytoplasm of baby hamster kidney cells. Treatment with a MAPK inhibitor redistributes CAS to the nucleus (49). Consistent with these effects, in the current study, CAS was found outside the nucleus, primarily along the nuclear periphery in VSMCs. This localization was not observed after treatment with 1 μM ceramide and was restored upon addition of 1 μM SB 202190, indicating that the redistribution of CAS was sensitive to p38 MAPK activation. A future priority is to determine whether CAS is a direct target for p38 MAPK activity or whether it achieves its effects through a secondary associated pathway.

CAS is the endogenous exporter of nuclear importin-α (50). In this study, ceramide pretreatment redistributed CAS, suggesting the relocalization of importin-α. Indeed, distinct nonnuclear localization of importin-α was observed. This would be expected to alter nucleocytoplasmic trafficking, as importin-α is critical in shuttling proteins to the nucleus (30). Changes in nucleocytoplasmic trafficking have direct consequences on rates of cellular growth (36), and cell counts as well as proliferative marker assays confirmed nonapoptotic decreases in cell numbers after ceramide treatment in the present study.

In summary, this study is the first to identify a sphingolipid metabolite with the capacity to induce robust inhibition of nuclear protein import mediated by a cytosolic signaling mechanism, demonstrating a previously unrecognized property of ceramide with physiological and pathological relevance. Ceramide orchestrates a variety of stress responses, including inflammation, cell differentiation, cell proliferation, atherosclerosis, thrombosis, apoptosis and vascular contractile function, through the activation of various signaling pathways (4, 51–53). Here, ceramide alters the smooth muscle cellular proliferative state, specifically through p38 MAPK-mediated redistribution of nucleocytoplasmic trafficking machinery. Further characterization of sphingolipid metabolic messengers, and their substrates, will facilitate the opportunity to ultimately identify novel therapeutic targets within the nuclear transport machinery (54) in the study of vascular cellular growth and its regulation.

This work was supported by grants from the Canadian Institutes of Health Research and the Natural Sciences and Engineering Research Council. The authors acknowledge the technical assistance of Janna M. Ellis and Nicole T. Gavel during this study.

REFERENCES

1. Merrill, A. H., Jr. 2002. De novo sphingolipid biosynthesis: a necessary, but dangerous, pathway. *J. Biol. Chem.* **277:** 25843–25846.
2. Hannun, Y. A., and L. M. Obeid. 2002. The ceramide-centric universe of lipid-mediated cell regulation: stress encounters of the lipid kind. *J. Biol. Chem.* **277:** 25847–25850.
3. Kolesnick, R., and Z. Fuks. 2003. Radiation and ceramide-induced apoptosis. *Oncogene.* **22:** 5897–5906.
4. Uchida, Y., A. D. Nardo, V. Collins, P. M. Elias, and W. M. Holleran. 2003. *De novo* ceramide synthesis participates in the ultraviolet B irradiation-induced apoptosis in undifferentiated cultured human keratinocytes. *J. Invest. Dermatol.* **120:** 662–669.
5. Johns, D. G., R. C. Webb, and J. R. Charpie. 2001. Impaired ceramide signalling in spontaneously hypertensive rat vascular smooth muscle: a possible mechanism for augmented cell proliferation. *J. Hypertens.* **19:** 63–70.
6. Conway, A., N. J. Pyne, and S. Pyne. 2000. Ceramide-dependent regulation of p42/p44 mitogen-activated protein kinase and c-Jun N-terminal-directed protein kinase in cultured airway smooth muscle cells. *Cell. Signal.* **12:** 737–743.
7. Feldherr, C. M., and D. Akin. 1993. Regulation of nuclear transport in proliferating and quiescent cells. *Exp. Cell Res.* **205:** 179–186.
8. Hood, J. K., and P. A. Silver. 2000. Diverse nuclear transport pathways regulate cell proliferation and oncogenesis. *Biochim. Biophys. Acta.* **1471:** M31–M41.
9. Jans, D. A., and S. Hubner. 1996. Regulation of protein transport to the nucleus: central role of phosphorylation. *Physiol. Rev.* **76:** 651–685.
10. Kehlenbach, R. H., and L. Gerace. 2000. Phosphorylation of the nuclear transport machinery down-regulates nuclear protein import in vitro. *J. Biol. Chem.* **275:** 17848–17856.
11. Adam, E. J., and S. A. Adam. 1994. Identification of cytosolic factors required for nuclear location sequence-mediated binding to the nuclear envelope. *J. Cell Biol.* **125:** 547–555.
12. Moore, M. S., and G. Blobel. 1992. The two steps of nuclear import, targeting to the nuclear envelope and translocation through the nuclear pore, require different cytosolic factors. *Cell.* **69:** 939–950.
13. Lyman, S. K., and L. Gerace. 2001. Nuclear pore complexes: dynamics in unexpected places. *J. Cell Biol.* **154:** 17–20.
14. Rout, M. P., J. D. Aitchison, A. Suprapto, K. Hjertaas, Y. Zhao, and B. T. Chait. 2000. The yeast nuclear pore complex: composition, architecture, and transport mechanism. *J. Cell Biol.* **148:** 635–651.
15. Ryan, K. J., and S. R. Wente. 2000. The nuclear pore complex: a protein machine bridging the nucleus and cytoplasm. *Curr. Opin. Cell Biol.* **12:** 361–371.
16. Robbins, J., S. M. Dilworth, R. A. Laskey, and C. Dingwall. 1991. Two interdependent basic domains in nucleoplasmin nuclear targeting sequence: identification of a class of bipartite nuclear targeting sequence. *Cell.* **64:** 615–623.
17. Adam, S. A., E. J. Adam, N. C. Chi, and G. D. Visser. 1995. Cytoplasmic factors in NLS-mediated targeting to the nuclear pore complex. *Cold Spring Harb. Symp. Quant. Biol.* **60:** 687–694.
18. Cingolani, G., H. A. Lashuel, L. Gerace, and C. W. Muller. 2000. Nuclear import factors importin alpha and importin beta undergo mutually induced conformational changes upon association. *FEBS Lett.* **484:** 291–298.
19. Gorlich, D., N. Pante, U. Kutay, U. Aebi, and F. R. Bischoff. 1996. Identification of different roles for RanGDP and RanGTP in nuclear protein import. *EMBO J.* **15:** 5584–5594.
20. Cingolani, G., C. Petosa, K. Weis, and C. W. Muller. 1999. Structure of importin-beta bound to the IBB domain of importin-alpha. *Nature.* **399:** 221–229.
21. Ben-Efraim, I., and L. Gerace. 2001. Gradient of increasing affinity

of importin beta for nucleoporins along the pathway of nuclear import. *J. Cell Biol.* **152:** 411–417.
22. Pemberton, L. F., G. Blobel, and J. S. Rosenblum. 1998. Transport routes through the nuclear pore complex. *Curr. Opin. Cell Biol.* **10:** 392–399.
23. Radu, A., G. Blobel, and M. S. Moore. 1995. Identification of a protein complex that is required for nuclear protein import and mediates docking of import substrate to distinct nucleoporins. *Proc. Natl. Acad. Sci. USA.* **92:** 1769–1773.
24. Azuma, Y., and M. Dasso. 2000. The role of Ran in nuclear function. *Curr. Opin. Cell Biol.* **12:** 302–307.
25. Lyman, S. K., T. Guan, J. Bednenko, H. Wodrich, and L. Gerace. 2002. Influence of cargo size on Ran and energy requirements for nuclear protein import. *J. Cell Biol.* **159:** 55–67.
26. Schwoebel, E. D., B. Talcott, I. Cushman, and M. S. Moore. 1998. Ran-dependent signal-mediated nuclear import does not require GTP hydrolysis by Ran. *J. Biol. Chem.* **273:** 35170–35175.
27. Kehlenbach, R. H., R. Assheuer, A. Kehlenbach, J. Becker, and L. Gerace. 2001. Stimulation of nuclear export and inhibition of nuclear import by a Ran mutant deficient in binding to Ran-binding protein 1. *J. Biol. Chem.* **276:** 14524–14531.
28. Moroianu, J. 1998. Distinct nuclear import and export pathways mediated by members of the karyopherin β family. *J. Cell. Biochem.* **70:** 231–239.
29. Faustino, R. S., L. N. Stronger, M. N. Richard, M. P. Czubryt, D. A. Ford, M. A. Prociuk, E. Dibrov, and G. N. Pierce. 2007. RanGAP-mediated nuclear protein import in vascular smooth muscle cells is augmented by lysophosphatidylcholine. *Mol. Pharmacol.* **71:** 438–445.
30. Behrens, P., U. Brinkmann, and A. Wellmann. 2003. CSE1L/CAS: its role in proliferation and apoptosis. *Apoptosis.* **8:** 39–44.
31. Maul, G. G., L. L. Deaven, J. J. Freed, G. L. Campbell, and W. Becak. 1980. Investigation of the determinants of nuclear pore number. *Cytogenet. Cell Genet.* **26:** 175–190.
32. Czubryt, M. P., J. A. Austria, and G. N. Pierce. 2000. Hydrogen peroxide inhibition of nuclear protein import is mediated by the mitogen-activated protein kinase, ERK2. *J. Cell Biol.* **148:** 7–16.
33. Massaeli, H., J. A. Austria, and G. N. Pierce. 1999. Chronic exposure of smooth muscle cells to minimally oxidized LDL results in depressed inositol 1,4,5-trisphosphate receptor density and Ca(2+) transients. *Circ. Res.* **85:** 515–523.
34. Jankowski, R., M. P. Czubryt, and G. N. Pierce. 2000. The nuclear protein import assay in vascular smooth muscle cells. *J. Pharmacol. Toxicol. Methods.* **44:** 421–427.
35. Faustino, R. S., D. C. Rousseau, M. N. Landry, A. L. Kostenuk, and G. N. Pierce. 2006. Effects of mitogen-activated protein kinases on nuclear protein import. *Can. J. Physiol. Pharmacol.* **84:** 469–475.
36. Richard, M. N., J. F. Deniset, A. L. Kneesh, D. Blackwood, and G. N. Pierce. 2007. Mechanical stretch stimulates smooth muscle cell growth, nuclear protein import and nuclear pore expression through mitogen-activated protein kinase activation. *J. Biol. Chem.* **282:** 23081–23088.
37. Solsbacher, J., P. Maurer, F. R. Bischoff, and G. Schlenstedt. 1998. Cse1p is involved in export of yeast importin α from the nucleus. *Mol. Cell. Biol.* **18:** 6805–6815.
38. Zettler, M. E., M. A. Prociuk, J. A. Austria, G. Zhong, and G. N. Pierce. 2004. Oxidized low-density lipoprotein retards the growth of proliferating cells by inhibiting nuclear translocation of cell cycle proteins. *Arterioscler. Thromb. Vasc. Biol.* **24:** 727–732.
39. Zettler, M. E., M. A. Prociuk, J. A. Austria, H. Massaeli, G. Zhong, and G. N. Pierce. 2003. OxLDL stimulates cell proliferation through a general induction of cell cycle proteins. *Am. J. Physiol. Cell Physiol.* **284:** H644–H653.
40. Sprott, K. M., M. J. Chumley, J. M. Hanson, and R. T. Dobrowsky. 2002. Decreased activity and enhanced nuclear export of CCAAT-enhancer-binding protein β during inhibition of adipogenesis by ceramide. *Biochem. J.* **365:** 181–191.
41. Siskind, L. J., and M. Colombini. 2000. The lipids C_2-and C_{16}-ceramide form large stable channels. *J. Biol. Chem.* **275:** 38640–38644.
42. Siskind, L. J., R. N. Kolesnick, and M. Colombini. 2002. Ceramide channels increase the permeability of the mitochondrial outer membrane to small proteins. *J. Biol. Chem.* **277:** 26796–26803.
43. Hla, T. 2003. Signaling and biological actions of sphingosine-1-phosphate. *Pharmacol. Res.* **47:** 401–407.
44. Spiegel, S., and S. Milstien. 2000. Sphingosine-1-phosphate: signaling inside and out. *FEBS Lett.* **476:** 55–57.
45. Spiegel, S., and S. Milstien. 2002. Sphingosine-1-phosphate, a key cell signaling molecule. *J. Biol. Chem.* **277:** 25851–25854.
46. Brinkmann, U., E. Brinkmann, M. Gallo, and I. Pastan. 1995. Cloning and characterization of a cellular apoptosis susceptibility gene, the human homologue to the yeast chromosome segregation gene *CSE1*. *Proc. Natl. Acad. Sci. USA.* **92:** 10427–10431.
47. Kutay, U., F. R. Bischoff, S. Kostka, R. Kraft, and D. Gorlich. 1997. Export of importin alpha from the nucleus is mediated by a specific nuclear transport factor. *Cell.* **90:** 1061–1071.
48. Scherf, U., I. Pastan, M. C. Willingham, and U. Brinkmann. 1996. The human CAS protein which is homologous to the CSE1 yeast chromosome segregation gene product is associated with microtubules and mitotic spindle. *Proc. Natl. Acad. Sci. USA.* **93:** 2670–2674.
49. Scherf, U., P. Kalab, M. Dasso, I. Pastan, and U. Brinkmann. 1998. The hCSE1/CAS protein is phosphorylated by HeLa extracts and MEK-1: MEK-1 phosphorylation may modulate the intracellular localization of CAS. *Biochem. Biophys. Res. Commun.* **250:** 623–628.
50. Görlich, D. 1997. Nuclear protein import. *Curr. Opin. Cell Biol.* **9:** 412–419.
51. Buccoliero, R., and A. H. Futerman. 2003. The roles of ceramide and complex sphingolipids in neuronal cell function. *Pharmacol. Res.* **47:** 409–419.
52. Castillo, S. S., and D. Teegarden. 2001. Ceramide conversion to sphingosine-1-phosphate is essential for survival in C3H10T1/2 cells. *J. Nutr.* **131:** 2826–2830.
53. Echten-Deckert, G. V., A. Klein, T. Linke, T. Heinemann, J. Weisgerber, and K. Sandhoff. 1997. Turnover of endogenous ceramide in cultured normal and Farber fibroblasts. *J. Lipid Res.* **38:** 2569–2579.
54. Faustino, R. S., T. J. Nelson, A. Terzic, and C. Perez-Terzic. 2007. Nuclear transport: target for therapy. *Clin. Pharmacol. Ther.* **81:** 880–886.